Global Stabilization of a Class of Uncertain Systems with Saturated Adaptive Robust Control *

J. Q. Gong, Bin Yao+

School of Mechanical Engineering
Purdue University, West Lafayette, IN 47907, USA
+ Tel: (765)494-7746 Fax:(765)494-0539
Email:{gong2, byao}@ecn.purdue.edu

Abstract

In this paper, a class of saturated adaptive robust control (SARC) laws are developed for nonlinear systems in the "chain-of-integrator" form with both parametric uncertainties and non-repeatable uncertainties. A guaranteed transient performance and final tracking accuracy is achieved in general. Furthermore, asymptotic output tracking is also achievable provided that the system undergoes parametric uncertainties only. Discontinuous projection method is used in the adaptation law for a controlled learning. Given the saturation limits of control authority, certain criteria are obtained to predict the achievable high-performance working range of the closed-loop system by taking into account the order of system, the bounds of both parametric uncertainties and non-repeatable nonlinearities, and the required performance, such as reaching time. At the same time, these criteria can also be used in the trajectory planning to obtain realizable desired trajectories. Consequently, an integrated design of achievable desired trajectory and control law may be achieved. The proposed SARC is then applied to the control of a linear motor drive system, and an excellent output tracking performance is obtained in experiments.

1 Introduction

The problem of stabilizing linear and nonlinear systems with saturated control has been extensively studied [1, 2, 3], which reflects the common concern that control authorities of actuators are in general limited. An excellent chronological bibliography on saturating actuators was given in [4]. In [1], a nested feedback design methodology was used to construct a saturated nonlinear globally asymptotically stabilizing state feedback control law for a chain of integrators of length n. More general cases were studied in [3]. A low-and-high gain method was used in [2, 5] to develop both state feedback and output feedback saturated control laws for linear systems. In all these works, only linear systems were considered and it was assumed that the systems are exactly known. However, in reality, there are always discrepancies between the design models and the actual systems. Parameters of systems may not be known exactly. Non-repeatable nonlinearities, such as disturbances, also affect the performance of systems. Thus, it is of practical benefits to be able to take into account all these uncertainties in the design explicitly.

As a stepping stone to deal with all the above practical issues, the adaptive robust control (ARC) design approach was proposed recently [6]. By using certain robust filter structures to attenuate the effect of model uncertainties, ARC achieves a guaranteed transient performance and final tracking accuracy in general. Simultaneously, parameter adaptation is employed to reduce the model uncertainties due to parametric uncertainties for an improved tracking performance (asymptotic output tracking for parametric uncertainties). These strong performance results achieved by ARC motivate us to investigate whether the essential idea of ARC can be used to construct a high performance saturated controller for uncertain systems.

In this paper, the nested saturated control design in [1] and the ARC approach in [6] are integrated to develop a class of SARC for "chain-of-integrator" systems which undergo both parametric uncertainties and non-repeatable nonlinearities. With a limited control effort, the proposed SARC preserves all the theoretical performance that an ARC can achieve if certain criteria are satisfied. These criteria reveal that the amount of control authority needed for global stabilization and performance depends on the system order, structural properties, the degree of model uncertainties, and the desired performance. The criteria also give some guidelines on how to choose a feasible desired trajectory for an uncertain system with limited control authority.

2 Problem Formulation

By considering both parametric uncertainties and unstructured uncertainties, the system discussed has the

*The work is supported by the National Science Foundation under the CAREER grant CMS-9734345

following so-called "chain-of-integrator" form

$$\begin{aligned} \dot{x}_i &= x_{i+1}, \quad i = 1, \cdots, n-1 \\ \dot{x}_n &= \phi^T(\mathbf{x}, t)\theta + u(t) + \Delta(\mathbf{x}, t) \end{aligned} \tag{1}$$

where $\mathbf{x} = [x_1, \cdots, x_n]^T$ is the system state vector, $\phi(\mathbf{x}, t) = [\phi_1(\mathbf{x}, t), \cdots, \phi_r(\mathbf{x}, t)]^T$ is the vector of known basis functions, $\theta = [\theta_1, \cdots, \theta_r]^T$ is the unknown constant parameter vector, r is the number of the unknown constant parameters, $\phi^T\theta$ denotes the structured nonlinearity with parametric uncertainties, $u(t)$ is the system input, and $\Delta(\mathbf{x}, t)$ represents the lumped *non-repeatable* unstructured nonlinearities such as disturbances. The following practical assumptions are made

Assumption 1
$\theta \in \Omega_\theta = \{\theta : \rho_{l,\theta_i} \le \theta_i \le \rho_{u,\theta_i},\ i = 1, 2, \cdots, r\}$, where ρ_{l,θ_i} and ρ_{u,θ_i} are the known lower and upper bound of θ_i, respectively.

Assumption 2 *$\sup_{\theta, \hat{\theta} \in \Omega_\theta}\{|\phi^T\tilde{\theta} - \Delta|\} \le h$, where $\hat{\theta} = [\hat{\theta}_1, \cdots, \hat{\theta}_r]^T$ represents the estimate of θ, $\tilde{\theta} = \hat{\theta} - \theta$ is the estimation error, and h is a known constant.*

In later derivation, denote $I_{\theta_i} = \rho_{u,\theta_i} - \rho_{l,\theta_i}$, and $\mathbf{I}_\theta = [I_{\theta_1}, \cdots, I_{\theta_r}]^T$. Suppose that the desired state trajectory is $\mathbf{x}_d(t) = [x_d, x_d^{(1)}, \cdots, x_d^{(n-1)}]^T$. *The control objective is to design a saturated control law for u such that the system state variable vector $\mathbf{x}$ tracks $\mathbf{x}_d$ as closely as possible.* Define $\tilde{\mathbf{x}}(t) = \mathbf{x}(t) - \mathbf{x}_d(t)$, and $\tilde{\mathbf{x}}$ satisfies

$$\begin{aligned} \dot{\tilde{x}}_i &= \tilde{x}_{i+1}, \quad i = 1, \cdots, n-1 \\ \dot{\tilde{x}}_n &= -x_d^{(n)} + \phi^T(\mathbf{x}, t)\theta + u(t) + \Delta(\mathbf{x}, t) \end{aligned} \tag{2}$$

3 Mathematical Preliminaries

Before developing the specific control law for (1), the following mathematical preliminaries are introduced.

3.1 Discontinuous projection mapping

Based on the bounds of parameters, a discontinuous projection mapping $\mathbf{Proj}(\bullet)$ can be defined as follows [7]

$$\mathbf{Proj}_{\hat{\theta}}(\bullet) = \left\{Proj_{\hat{\theta}}(\bullet_i)\right\} \tag{3}$$

with its i-th element being

$$Proj_{\hat{\theta}}(\bullet_i) = \begin{cases} 0 & if \begin{cases} \hat{\theta}_i = \rho_{u,\theta_i} \text{ and } \bullet_i > 0 \\ \quad or \\ \hat{\theta}_i = \rho_{l,\theta_i} \text{ and } \bullet_i < 0 \end{cases} \\ \bullet_i & otherwise \end{cases} \tag{4}$$

Through the use of projection mapping, the following nice properties can be obtained [6]

P1. Each component of parameter estimate is always within its known bound, i.e.,

$$\rho_{l,\theta_i} \le \hat{\theta}_i \le \rho_{u,\theta_i}, \qquad i = 1, \cdots, r \tag{5}$$

P2. In addition, the following inequality holds

$$\tilde{\theta}^T(\Gamma_\theta^{-1}\mathbf{Proj}_{\hat{\theta}}(\Gamma_\theta \bullet) - \bullet) \le 0, \quad \forall \bullet \tag{6}$$

where Γ_θ is a constant diagonal positive definite matrix.

Remark 1 *Property P1 (5) shows that the estimates of parameters are always within their known ranges, and the bound of the estimate error is $||\tilde{\theta}|| \le ||\mathbf{I}_\theta||$. With this nice property, Assumption 2 becomes reasonable and practical.*

3.2 Saturation function

Definition 1 *[1] Given two positive constants, L and M with $L < M$, a function $\sigma : \mathcal{R} \to \mathcal{R}$ is said to be a linear saturation function of (L, M), if it is a continuous, nondecreasing function satisfying: 1. $s\sigma(s) > 0$, $\forall s \ne 0$; 2. $\sigma(s) = s$ when $|s| < L$; 3. $|\sigma(s)| \le M$, $\forall s \in \mathcal{R}$.*

4 SARC Design

In order to develop SARC, it is more convenient to transform system coordinates $\tilde{\mathbf{x}}$ to $\mathbf{y}$ by the linear transformation $\mathbf{y} = \mathbf{T}\tilde{\mathbf{x}}$ with $\mathbf{T} = \{T_{ij}\}$ being given as follows

$$\begin{aligned} &T_{i,n} = 1, && 1 \le i \le n \\ &T_{n,j} = 0, && 1 \le j \le n-1 \\ &T_{i,j} = \textstyle\sum_{m=i+1}^{n} k_m T_{m,j+1}, && 1 \le i, j \le n-1 \end{aligned} \tag{7}$$

and $k_m,\ m = 1, \cdots, n$ being the positive constant design parameters. The state equations (2) are then transformed to

$$\begin{aligned} \dot{y}_i &= k_{i+1}y_{i+1} + \cdots + k_n y_n - x_d^{(n)} + \phi^T\theta + \Delta + u, \\ &\qquad i = 1 \cdots, n-1 \\ \dot{y}_n &= -x_d^{(n)} + \phi^T\theta + \Delta + u \end{aligned} \tag{8}$$

Remark 2 *It can be verified that the above transformation leads to*

$$\begin{aligned} y_i &= \textstyle\prod_{m=i+1}^{n}(\frac{d}{dt} + k_m)\tilde{x}_i, \quad i = 1, \cdots, n-1 \\ y_n &= \tilde{x}_n \end{aligned} \tag{9}$$

Thus, the transfer functions from y_i to $\tilde{x}_i$ are

$$\frac{\bar{x}_i(s)}{y_i(s)} = \frac{1}{\prod_{m=i+1}^{n}(s + k_m)}, \quad i = 1, \cdots, n-1 \tag{10}$$

Consider the control law

$$\begin{aligned} u &= \sigma_{n+1}\left(u_a - u_{s_n}\right) \\ u_a &= x_d^{(n)} - \phi^T\hat{\theta} \\ u_{s_i} &= \sigma_i\left(k_i y_i + u_{s_{i-1}}\right), \quad i = n, \cdots, 2 \\ u_{s_1} &= \sigma_1\left(k_1 y_1\right) \end{aligned} \tag{11}$$

where the parameter $\{L_i, M_i\}$ of σ_i satisfies

$$|x_d^{(n)} - \phi^T\hat{\theta}| \le L_{n+1} - M_n \tag{12}$$

$$L_{i+1} \ge h + 2M_i + \eta_{i+1},\ i = 0, \cdots, n-1 \tag{13}$$

with $\eta_i \ge 0$, $i = 1, \cdots, n$, and $M_0 = 0$.

Theorem 4.1 *With SARC (11) satisfying conditions (12)-(13), all signals are bounded. Furthermore, the tracking error* $\tilde{\mathbf{x}}$ *reaches a designed region in a finite time and stays within that region thereafter.* ♢

Proof. Noting condition (12) and property 3 of Definition 1, it follows that $|x_d^{(n)} - \phi^T\hat{\theta} - \sigma_n(\cdots)| \leq |x_d^{(n)} - \phi^T\hat{\theta}| + |\sigma_n(\cdots)| \leq L_{n+1} - M_n + M_n = L_{n+1}$. Hence, σ_{n+1} works in its linear range, i.e., $\sigma_{n+1}(\cdot) = \cdot$. Thus, SARC (11) is equivalent to $u = u_a - u_{s_n}$, and the system state equations in (8) become

$$\begin{aligned} \dot{y}_i &= k_{i+1}y_{i+1} + \cdots + k_n y_n - \phi^T\tilde{\theta} + \Delta - u_{s_n}, \\ & \qquad\qquad i = 1, \cdots, n-1 \\ \dot{y}_n &= -\phi^T\tilde{\theta} + \Delta - u_{s_n} \end{aligned} \tag{14}$$

Firstly, let us check the evolution of the state y_n. Consider the positive definite function $V_n = \frac{1}{2}y_n^2$. By using the last equation in (14), the time derivative of V is

$$\dot{V}_n = y_n\dot{y}_n = y_n(-\phi^T\tilde{\theta} + \Delta) - y_n u_{s_n} \tag{15}$$

It will be shown that y_n converges to the region $\Omega_{y_n} = \{y_n : |y_n| \leq \frac{h + M_{n-1} + \eta_n}{k_n}\}$ in a finite time as follows.

Suppose that $y_n \notin \Omega_{y_n}$, i.e.,

$$|k_n y_n| > h + M_{n-1} + \eta_n \tag{16}$$

Since $|\sigma_{n-1}| \leq M_{n-1}$ and $k_n > 0$, (16) leads to

$$\begin{aligned} \text{sign}(y_n) &= \text{sign}(k_n y_n + u_{s_{n-1}}) \\ &= \text{sign}(\sigma_n(k_n y_n + u_{s_{n-1}})) \end{aligned} \tag{17}$$

From (16), it results that

$$\begin{aligned} & |k_n y_n + \sigma_{n-1}(\cdots)| \geq |(|k_n y_n| - |\sigma_{n-1}(\cdots)|)| \\ > \;& h + M_{n-1} + \eta_n - M_{n-1} = h + \eta_n \end{aligned} \tag{18}$$

Since σ_n is nondecreasing, $h + \eta_n \leq L_n$, and σ_n works in its linear range, (18) implies

$$|\sigma_n(k_n y_n + \sigma_{n-1}(\cdots))| > h + \eta_n \tag{19}$$

Thus, from equations (15) and (17), Assumption 2, and inequality (19), it follows that

$$\begin{aligned} \dot{V}_n &= y_n(-\phi^T\tilde{\theta} + \Delta) - y_n\sigma_n(k_n y_n + u_{s_{n-1}}) \\ &= y_n(-\phi^T\tilde{\theta} + \Delta) - |y_n|\text{sign}(y_n)\sigma_n(k_n y_n + u_{s_{n-1}}) \\ &= y_n(-\phi^T\tilde{\theta} + \Delta) - |y_n||\sigma_n(k_n y_n + u_{s_{n-1}})| \\ &< |y_n|h - |y_n|(h + \eta_n) = -\eta_n|y_n| = -\eta_n\sqrt{2V_n} \end{aligned} \tag{20}$$

which implies that [8]

$$|y_n(t)| - |y_n(0)| < -\eta_n t \tag{21}$$

Suppose that $y_n(0) \notin \Omega_{y_n}$. Let $t_{r,n}$ denote the time that y_n reaches the boundary. From (21), the upper bound of the reaching time is obtained

$$t_{r,n} < \frac{|y_n(0)| - \frac{h + M_{n-1} + \eta_n}{k_n}}{\eta_n} \tag{22}$$

This proves that y_n converges to the region Ω_{y_n} in a finite time and will stay within the region thereafter.

Since $y_n \in \Omega_{y_n}$ in a finite time, the condition (13) implies that $|k_n y_n + \sigma_{n-1}(\cdots)| \leq h + M_{n-1} + \eta_n + M_{n-1} \leq L_n$, which indicates that σ_n works in its linear range in a finite time. Furthermore, due to the boundednesses of $-\phi^T\tilde{\theta} + \Delta$ and σ_i, from (14), it can be recursively checked that $y_{n-1}, \cdots, y_1$ are bounded in any finite time.

Now consider the evolution of y_{n-1}. Observe that σ_n now works in the linear range. Hence, the dynamic equation of y_{n-1} becomes

$$\begin{aligned} \dot{y}_{n-1} &= k_n y_n - \phi^T\tilde{\theta} + \Delta - k_n y_n - u_{s_{n-1}} \\ &= -\phi^T\tilde{\theta} + \Delta - u_{s_{n-1}} \end{aligned} \tag{23}$$

Same as before, y_{n-1} will enter the region $\Omega_{y_{n-1}} = \{y_{n-1} : |y_{n-1}| \leq \frac{h + M_{n-2} + \eta_{n-1}}{k_{n-1}}\}$ in a finite time and stay in the region thereafter, and other states $y_1, \cdots, y_{n-2}$ remain bounded. The upper bound of the reaching time of y_{n-1} is $t_{r,n} + \max\left\{\frac{|y_{n-1}(t_{r,n})| - \frac{h + M_{n-2} + \eta_{n-1}}{k_{n-1}}}{\eta_{n-1}}, 0\right\}$, where $y_{n-1}(t_{r,n})$ is the value of y_{n-1} at $t_{r,n}$.

By induction, all the σ_i's will work in the linear ranges in a finite time. The total reaching time satisfies

$$\begin{aligned} t_{total} &= t_{r,1} \leq \sum_{i=1}^{n-1} \max\left\{\frac{|y_i(t_{r,i+1})| - \frac{h + M_{i-1} + \eta_i}{k_i}}{\eta_i}, 0\right\} \\ &\quad + \max\left\{\frac{|y_n(0)| - \frac{h + M_{n-1} + \eta_n}{k_n}}{\eta_n}, 0\right\} \end{aligned} \tag{24}$$

Hence, after a finite time interval t_{total}, (14) changes to

$$\dot{\mathbf{y}} = \mathbf{A}\mathbf{y} + \mathbf{B}(-\phi^T\tilde{\theta} + \Delta) \tag{25}$$

where

$$\mathbf{A} = \begin{bmatrix} -k_1 & 0 & \cdots & 0 & 0 \\ -k_1 & -k_2 & \ddots & 0 & 0 \\ \vdots & \vdots & \ddots & \ddots & \vdots \\ -k_1 & -k_2 & \cdots & -k_{n-1} & 0 \\ -k_1 & -k_2 & \cdots & -k_{n-1} & -k_n \end{bmatrix}, \mathbf{B} = \begin{bmatrix} 1 \\ \vdots \\ 1 \end{bmatrix} \tag{26}$$

Since matrix $\mathbf{A}$ is an exponentially stable matrix, and $\mathbf{B}(-\phi^T\tilde{\theta} + \Delta)$ is bounded, $\mathbf{y}$ is bounded. Due to the fact $\mathbf{y} = \mathbf{T}\tilde{\mathbf{x}}$, the tracking error $\tilde{\mathbf{x}}$ will also stay within a desirable region in a finite time. □

Remark 3 *Theorem 4.1 reveals that the tracking error will reach a designed region in a finite time, and the upper bound of* t_{total} *changes with* η_i*'s. Thus, a guaranteed transient performance is achieved. At the same time, sizes of regions* Ω_{y_i} *can also be tuned by changing* k_i*'s properly. In this sense, a guaranteed final tracking accuracy is obtained. Since* $|y_1| \leq \frac{h + \eta_1}{k_1}$ *(note that*

$M_0 = 0$) in a finite time, from the transfer function (10), $|\tilde{x}_1| \leq \frac{h+\eta_1}{\prod_{m=1}^{n} k_m}$ in a finite time [8]. It can also be proved that $|\tilde{x}_i| \leq \frac{h+M_{i-1}+\eta_i}{\prod_{m=i}^{n} k_m}$, $i = 1, \cdots, n$ in a finite time [8].

Remark 4 *Based on the condition (13), Definition 1 and $M_0 = 0$, by induction, it can be proved that*

$$L_n \quad > \quad (2^n - 1)h + \sum_{i=0}^{i=n-1} 2^i \eta_{n-i} \tag{27}$$

which indicates that the lower bound of M_n depends on the complexity of the system (order of the system, n), the degree of model uncertainties (h), and the desired performance (η_i). In viewing (12), the class of the desired trajectories is thus limited once the control authority bound L_{n+1} is given. The result of (27) can also be combined with (12) to obtain conditions that a feasible desired trajectory has to satisfy, which may be very useful in the desired trajectory planning stage. For example, a conservative upper bound for the $n-th$ derivative of a feasible desired trajectory can be obtained as

$$|x_d^{(n)}| \quad \leq \quad L_{n+1} - max\{|\phi^T \hat{\theta}|\} - M_n \tag{28}$$

Remark 5 *From equation (25), without considering model uncertainties, the characteristic equation of the closed-loop system is given by*

$$(\lambda + k_1)(\lambda + k_2) \cdots (\lambda + k_n) = 0 \tag{29}$$

Theoretically, k_i can be chosen arbitrarily large for a good tracking performance. In practice, they should be chosen based on the nature of the neglected dynamics such as the bandwidth of the actuators and the sampling time due to the digital implementation.

Since $\mathbf{A}$ in (26) is exponentially stable, the following Lyapunov equation

$$\mathbf{A}^T\mathbf{P} + \mathbf{P}\mathbf{A} = -\mathbf{Q} \tag{30}$$

has a symmetric positive definite (s.p.d.) solution $\mathbf{P}$ for any s.p.d. matrix $\mathbf{Q}$. Suppose that $\mathbf{Q}$ is given, and $\mathbf{P}$ is the solution to (30). The following adaptation law is proposed

$$\dot{\hat{\theta}} = \mathbf{Proj}_{\hat{\theta}}(\Gamma_\theta \phi \mathbf{B}^T \mathbf{P}\mathbf{y}) \tag{31}$$

where Γ_θ is a constant diagonal positive definite matrix representing the adaptation rate.

Theorem 4.2 *With SARC (11) satisfying conditions (12) and (13) and the use of adaptation law (31), asymptotic output tracking is achieved if non-repeatable nonlinearities Δ disappear in a finite time t_0, i.e., $\Delta \equiv 0$, $\forall t \geq t_0$.* ♢

Proof. From Theorem 4.1, it is known that in a finite time, the closed-loop system is described by

$$\dot{\mathbf{y}} = \mathbf{A}\mathbf{y} + \mathbf{B}(-\phi^T \tilde{\theta}) \tag{32}$$

where $\Delta \equiv 0$ is used, and $\mathbf{A}$ and $\mathbf{B}$ are given in (26).

Let $V = \frac{1}{2}\left(\mathbf{y}^T\mathbf{P}\mathbf{y} + \tilde{\theta}^T\Gamma_\theta^{-1}\tilde{\theta}\right)$. By using the adaptation law (31) and property (6), the time derivative of V is given by $\dot{V} = \frac{1}{2}\mathbf{y}^T\mathbf{Q}\mathbf{y} - \mathbf{y}^T\mathbf{P}\mathbf{B}\phi^T\tilde{\theta} + \tilde{\theta}^T\Gamma_\theta^{-1}\mathbf{Proj}_{\hat{\theta}}(\Gamma_\theta\phi\mathbf{B}^T\mathbf{P}\mathbf{y}) \leq -\frac{1}{2}\mathbf{y}^T\mathbf{Q}\mathbf{y} \leq 0$. Using the standard arguments in adaptive control [8], $\mathbf{y}$ goes to zero asymptotically. Hence, asymptotic output tracking is achieved. □

Remark 6 *Theorem 4.2 shows that, in the ideal case when the system is of parametric uncertainties only, the proposed SARC is able to eliminate the effect of model uncertainties completely and a better final tracking performance is achieved compared to its non-adaptation counterpart.*

Remark 7 *In the previous study, the input gain is 1. If the last equation of (1) changes to*

$$\dot{x}_n = \phi^T(\mathbf{x}, t)\theta + bu(t) + \Delta(\mathbf{x}, t) \tag{33}$$

with $b \neq 0$, SARC (11) then changes to

$$u = \frac{1}{b}\sigma_{n+1}\left(u_a - u_{s_n}\right) \tag{34}$$

All the previous results and remarks are still valid.

5 Experimental Studies

In this section, the proposed SARC will be applied to the control of a linear motor drive system.

5.1 Design model of linear motor drive systems

The system setup is given in Fig. 1, which is the same as that in [9]. In the experiments, the sampling frequency $f_s = 2.5\ kHz$, and the encoder resolution is $\pm 1\ \mu m$.

The design model of the linear motor drive system is given as follows

$$m\ddot{x} = u - B\dot{x} - f_p \text{psgn}(\dot{x}) - f_n \text{nsgn}(\dot{x}) + d_0 + \tilde{d} \tag{35}$$

where x is the position of the inertia load, m is the normalized* mass of the inertia load plus the coil assembly, u is the input voltage to the motor, B is an equivalent viscous friction coefficient of the system, $f_p\text{psgn}(\dot{x})$ and $f_n\text{nsgn}(\dot{x})$ are used to capture the main effects of the nonlinear friction, constant d_0 represents the average effect of model uncertainties, and $\tilde{d}$ is used to capture other effects of model uncertainties. It is assumed

*Normalized with respect to the unit of input voltage.

that B, f_p, f_n, and d_0 are unknown constants, and $\tilde{d}$ is bounded. By the off-line system identification, the value of m is obtained as 0.027. Functions psgn($\dot{x}$) and nsgn($\dot{x}$) are defined as follows

$$\text{psgn}(\dot{x}) = \begin{cases} 1 & \dot{x} > 0 \\ 0 & \dot{x} \le 0 \end{cases} \quad \text{nsgn}(\dot{x}) = \begin{cases} 0 & \dot{x} \ge 0 \\ -1 & \dot{x} < 0 \end{cases} \tag{36}$$

Dividing both sides of (35) by m, the design model (35) can be written into the form (1) with its last equation replaced by (33) and $n = 2$, $\phi(\mathbf{x}, t) = [-\dot{x}, -\text{psgn}(\dot{x}), -\text{nsgn}(\dot{x}), 1]^T$, $\theta = [\frac{B}{m}, \frac{f_p}{m}, \frac{f_n}{m}, \frac{d_0}{m}]^T$, $b = \frac{1}{m}$, and $\Delta(\mathbf{x}, t) = \frac{\tilde{d}}{m}$.

5.2 SARC and adaptation law

Following the SARC design in Section 4, we have

$$y_1 = k_2\tilde{x}_1 + \tilde{x}_2, \quad y_2 = \tilde{x}_2 \tag{37}$$

Correspondingly, SARC (34) has the following form

$$u = -m\sigma_3(\ddot{x}_d - \phi^T\hat{\theta} + \sigma_2(k_2\tilde{y}_2 + \sigma_1(k_1 y_1))) \tag{38}$$

In the experiments, $\sigma(x)$ is specified as follows

$$\sigma(x) = \begin{cases} x & |x| \le L \\ \sum_{i=0}^{3} a_i x^{3-i} & L < x < L + \epsilon_l \\ M & x \ge L + \epsilon_l \\ \sum_{i=0}^{3} (-1)^i a_i x^{3-i} & -L - \epsilon_l < x < -L \\ -M & x \le -L - \epsilon_l \end{cases} \tag{39}$$

where ϵ_l is the margin between the linear working range and the maximal control effort, and a_i, $i = 0, \cdots, 3$ are

$$\begin{aligned} a_0 &= \tfrac{1}{\epsilon_l^3}(2L - 2M + \epsilon_l) \\ a_1 &= -\tfrac{1}{\epsilon_l^3}(6L^2 + 6L\epsilon_l - 6ML - 3M\epsilon_l + 2\epsilon_l^2) \\ a_2 &= \tfrac{L+\epsilon_l}{\epsilon_l^3}(6L^2 - 6ML + 3L\epsilon_l + \epsilon_l^2) \\ a_3 &= -\tfrac{L^2}{\epsilon_l^3}(2L^2 + 4L\epsilon_l - 2ML - 3M\epsilon_l + 2\epsilon_l^2) \end{aligned} \tag{40}$$

which make sure that function $\sigma(x)$ is smooth up to its first derivative.

By using the above formula, one example of the saturation function is shown in Fig. 2 with $L = 10$, $\epsilon_l = 10$, and $M = L + \epsilon_l$. The linear working range is within the dashed square. The smooth joining ranges are within the two dotted rectangles, respectively. The remaining parts are the saturated parts, where the outputs of the function assume the maximal or minimal values.

With $\mathbf{Q} = \mathbf{I}$, solving (30) yields $P_{11} = \frac{k_1^2 + k_1k_2 + k_2^2}{2k_1k_2(k_1+k_2)}$, $P_{12} = P_{21} = -\frac{k_1}{2k_2(k_1+k_2)}$, and $P_{22} = \frac{1}{2k_2}$. Subsequently, the adaptation law (31) changes to

$$\dot{\hat{\theta}} = \mathbf{Proj}_{\hat{\theta}}\left\{\Gamma_\theta \phi \left[(P_{11} + P_{21})\, y_1 + (P_{12} + P_{22})\, y_2\right]\right\} \tag{41}$$

5.3 Design parameters

Parameters for control law are given as: $k_1 = k_2 = 400$; $h = 9$; $\eta_i = 10$, $i = 1, 2, 3$; $\epsilon_l = 10$ for all saturation functions; $L_i = h + 2M_{i-1} + \eta_i$, $M_i = L_i + \epsilon_l$, $i = 1, 2, 3$, and $M_0 = 0$.

Parameters for adaptation law are given as: $\Gamma_\theta = diag[10^7, 10^5, 10^5, 1.5 \times 10^8]$, $0.1 \le \hat{\theta}_1 \le 0.3$, $0 \le \hat{\theta}_2 \le 0.2$, $0 \le \hat{\theta}_3 \le 0.2$, and $-7 \le \hat{\theta}_4 \le 7$.

5.4 Experimental results

The desired trajectory is a point-to-point back-and-forth movement, whose position, velocity, and acceleration of the initial several periods are given in Fig. 3. The experimental results under the proposed SARC are given in Fig.4-6. In Fig. 4, it can be seen that the tracking error converges to a small region very quickly. Actually, the tracking error mainly stays within the measurement resolution most of time (shown by dashed lines in the figure), which illustrates the high performance of the proposed SARC. The estimates of parameters are given in Fig. 5. It can be seen that by using the projection mapping, all estimates are within their prescribed ranges (the two dashed lines in the fourth plot of Fig. 5 represents ± 7, respectively). A controlled learning is then achieved. The control input is given in Fig. 6, which is clearly bounded. The above results indicate that the proposed SARC can achieve a high performance if the total effects of the desired trajectory and all the uncertainties are within the linear working range of the system.

6 Conclusion

A class of SARC laws have been developed for nonlinear systems in the "chain-of-integrator" form with both parametric uncertainties and non-repeatable uncertainties. Discontinuous projection based adaptation law has been used to make sure that parameter estimates are tuned within a prescribed range. By doing so, a controlled learning has been achieved and the possible destabilizing effect of on-line adaptation could be avoided. A saturated ARC law was then constructed with an emphasis on performance in addition to global stabilization. Specifically, given the bound of control authority, with certain criteria satisfied, the proposed SARC is able to achieve a guaranteed output tracking transient performance and final tracking accuracy in general. In addition, in the presence of parametric uncertainty only, the control law is also able to achieve asymptotic output tracking. A by-product of the design is that the obtained criteria may also be used in the trajectory plan to construct realizable desired trajectories for nonlinear systems with uncertainties. The proposed SARC has been applied to the control a linear motor drive system, and excellent output tracking performance has been observed in experiments.

References

[1] A. R. Teel, "Global stabilization and restricted tracking for multiple integrators with bounded controls," *Systems and Control letters*, vol. 18, pp. 165–171, 1992.

[2] A. Saberi, Z. Lin, and A. R. Teel, "Control of linear

systems with saturating actuators," *IEEE Transactions on Automatic Control*, vol. 41, no. 3, pp. 368–378, 1996.

[3] H. J. Sussmann, E. D. Sontag, and Y. Yang, "A general result on the stabilization of linear systems using bounded controls," *IEEE Transactions on Automatic Control*, vol. 39, no. 12, pp. 2411–2425, 1994.

[4] D. S. Bernstein and A. N. Michel, "A chronological bibliography on saturating actuators," *International Journal of Robust and Nonlinear Control*, vol. 5, pp. 375–380, 1995.

[5] Z. Lin and A. Saberi, "A semi-global low-and-high gain design technique for linear systems with input saturation–stabilization and disturbance rejection," *International Journal of Robust and Nonlinear Control*, vol. 5, pp. 381–398, 1995.

[6] B. Yao and M. Tomizuka, "Adaptive robust control of SISO nonlinear systems in a semi-strict feedback form," *Automatica*, vol. 33, no. 5, pp. 893–900, 1997. (Part of the paper appeared in Proc. of 1995 American Control Conference, pp2500-2505).

[7] S. Sastry and M. Bodson, *Adaptive Control: Stability, Convergence and Robustness*. Englewood Cliffs, NJ 07632, USA: Prentice Hall, Inc., 1989.

[8] J. J. E. Slotine and W. Li, *Applied nonlinear control*. Englewood Cliffs, New Jersey: Prentice Hall, 1991.

[9] J. Q. Gong and B. Yao, "Neural network adaptive robust control with application to precision motion control of linear motors," *International Journal of Adaptive Control and Signal Processing*, 2000 (Accepted for the special issue on Developments in Intelligent Control for Industrial Applications).

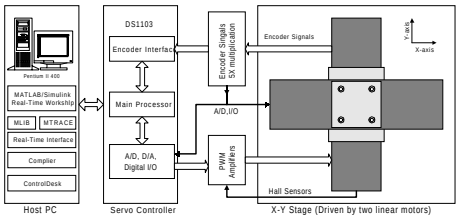

Figure 1: Experiment Setup

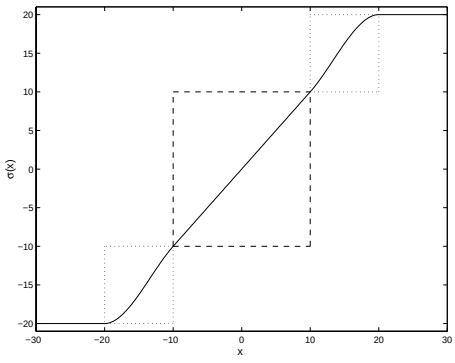

Figure 2: One example of saturation function

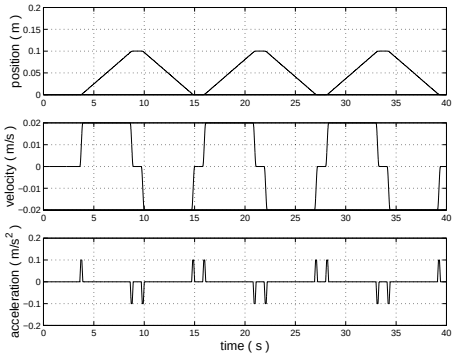

Figure 3: Position, velocity, and acceleration of the desired trajectory

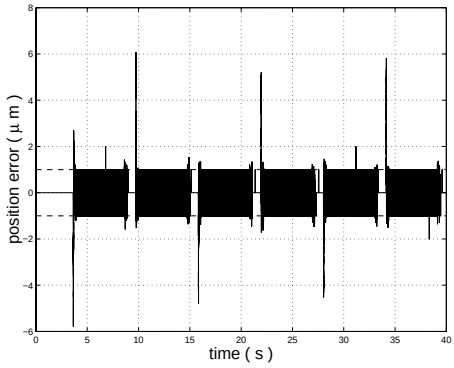

Figure 4: Position error under SARC

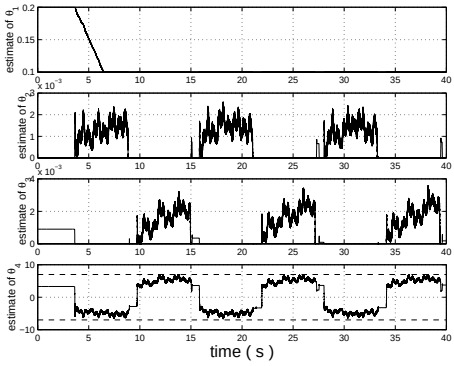

Figure 5: Estimate of θ under SARC

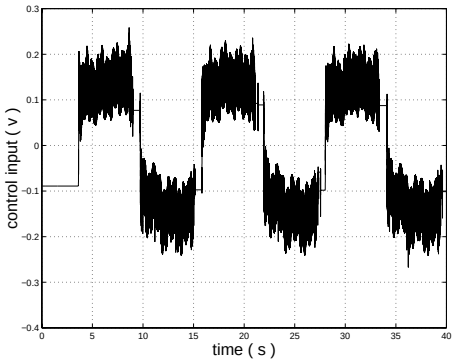

Figure 6: Control input under SARC